

## **DETERMINATION OF MICROSTRUCTURAL CHANGES BY SEVERELY PLASTICALLY DEFORMED COPPER-ALUMINUM ALLOY: OPTICAL STUDY**

N. Romčević<sup>1\*</sup>, M. Gilić<sup>1</sup>, I. Anžel<sup>2</sup>, R. Rudolf<sup>2,3</sup>, M. Mitrić<sup>4</sup>, M. Romčević<sup>1</sup>, B. Hadžić<sup>1</sup>,  
D. Joksimović<sup>5</sup>, M. Petrović Damjanović<sup>1</sup>, M. Kos<sup>2,6</sup>

<sup>1</sup> University of Belgrade, Institute of Physics, Belgrade, Serbia; <sup>2</sup> University of Maribor, Faculty of Mechanical Engineering, Slovenia; <sup>3</sup> Zlatarna Celje d.d., Slovenia; <sup>4</sup> Institute Vinca, University of Belgrade, Belgrade, Serbia; <sup>5</sup> Megatrend University, Belgrade, Serbia; <sup>6</sup> Sykofin d.o.o., Maribor, Slovenia

*(Received 21 January 2014; accepted 17 March 2014)*

### **Abstract**

*Our work deals with the problem of producing a complex metal-ceramic composite using the processes of internal oxidation (IO) and severe plastic deformation. For this purpose, Cu-Al alloy with 0.4wt.% of Al was used. IO of sample serves in the first step of the processing as a means for attaining a fine dispersion of nanosized oxide particles in the metal matrix. Production technology continues with repeated application of severe plastic deformation (SPD) of the resulting metal-matrix composite to produce the bulk nanoscaled structural material. SPD was carried out with equal channel angular pressing (ECAP), which allowed that the material could be subjected to an intense plastic strain through simple shear. Microstructural characteristics of one phase and multiphase material was studied on internally oxidized Cu with 0.4wt.% of Al sample composed of one phase copper-aluminum solid solution in the core and fine dispersed oxide particles in the same matrix in the mantle region. In this manner AFM, X-ray diffraction and Raman spectroscopy were used. Local structures in plastically deformed samples reflect presence of Cu, CuO, Cu<sub>2</sub>O, Cu<sub>4</sub>O<sub>3</sub> or Al<sub>2</sub>O<sub>3</sub> structural characteristics, depending on type of sample.*

**Key words:** *metals; oxides; atomic force microscopy; Raman spectroscopy; microstructure.*

### **1. Introduction**

An attractive and viable approach for improving the strength of copper is to introduce fine Al<sub>2</sub>O<sub>3</sub> particles into the Cu matrix, resulting in an oxide dispersion strengthening of the alloys (ODS alloy). A copper matrix containing fine nano-sized particles is attractive for its excellent combinations of thermal and electrical conductivity and overall microstructural stability. Internal oxidation (IO) can be used in order to achieve the fine Al<sub>2</sub>O<sub>3</sub> particles in the Cu matrix.

Internal oxidation (IO) is a diffusion-controlled process involving selective reactions of a less noble solute or second phase particles with oxygen (also nitrogen or carbon) diffusing in from the surface. The phenomenon is well understood for single phase solid solutions and can be interpreted according to the known theoretical models. From a technological standpoint the process can be used for oxide dispersion strengthening of alloys (ODS alloy) which retain improved mechanical properties at high temperatures [1]. Tensile strength of ODS alloys can be improved additionally by severe plastic

deformation, which can be achieved with equal channel angular pressing (ECAP), Figure 1 [2]. The ECAP process is a novel technique for producing ultra-fine grain structures on the submicron level by introducing a large amount of shear strain into the materials without changing the billet shape or dimensions [3]. Previous research on grain refinement and microstructural characteristics during the ECAP process are based mainly on one phase materials such as Cu and Al [4-6].

The influence of oxides or precipitates on the microstructural characteristic during the ECAP process has been investigated rarely. In fact the combination of IO and the ECAP process has not yet been studied and no information is available.

This paper describes the influence of the ECAP process on the microstructural characteristic of one phase and multiphase materials. The microstructural features in one phase and multiphase material were studied on partially internally oxidized Cu-0.4wt.%Al sample, composed of one phase copper-aluminum solid solution in the core and fine dispersed oxide particles in the same matrix in the mantle region.

---

\* Corresponding author: romcevi@ipb.ac.rs

## 2. Experimental

IO of the samples was used in the first step of processing to attain a fine dispersion of nano-sized oxide particles in the metal matrix. Furthermore, the second step, the repeated application of severe plastic deformation of the resulting metal-ceramic composites is applied as an effective technique for producing bulk nano-scaled structures [7].

The experiments have been performed using a sample of internally oxidized Cu-0.4 wt.% Al alloy. Billet cross-sections of 10 x10 mm<sup>2</sup> and 50 mm in length were made by vacuum melting, mold casting and calibration rolling. Billets were then homogenized for 1 hour at 1173K. The IO procedure was performed in a mixture of equal parts of copper oxide and copper metal powders enclosed in a glass ampule and held at 1173K for 72 hours in a tube furnace. This procedure allowed a partial pressure of oxygen to be equal to the decomposition pressure of copper oxide and maintained the saturation concentration of oxygen in the surface of the billet.

Within our research we have designed our own ECAP tool. Many parameters had to be taken into consideration regarding billet shape, size and maximum work load. We decided to use a 90° die with a square section of 10 x 10 mm<sup>2</sup> cross-section and billet length of 50mm. The outer radius of curvature was 1mm. The die, which consisted of two blocks which were bolted together to give a single internal channel and the piston, were made from UTOP Mo1 tool steel, hardened to approximately 61 HRC. A simple standard press with 60 metric tons capacity was used. The ECAP pressings were carried out at room temperature using a route where the billet is rotated by 90° in alternate directions. The billet was pressed four times through the ECAP die.

The samples were taken transversely (x plane) and longitudinally (y plane) to the pressing direction after each step of technological process, as shown in Figure 1, and demonstrated schematically in other Figures.

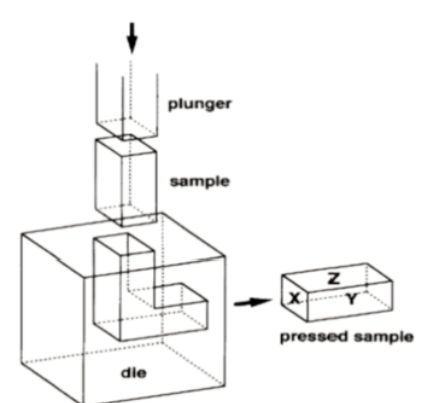


Figure 1. Schematic illustration of equal channel angular pressing (ECAP)

From each plane two samples were taken, one from the mantle region and one from the core.

Microstructural characterization was carried out by AFM, X-ray diffraction and Raman spectroscopy. The samples for measurements were prepared with standard metallographic preparation methods using mechanical polishing with 0.05 μm alumina and etched with FeCl<sub>3</sub>+HCl.

## 3. Results and discussion

### 3.1. AFM measurements

The technological process was observed with AFM. Results for samples taken transversely to the pressing direction are shown in Figure 2, and for samples taken longitudinally to the pressing direction are shown in Figure 3. The place where the samples were taken from and the steps of the technological process are presented in these Figures too. Figures 2a and 3a feature samples taken from the original alloy after the homogenization. The consequences of rolling are seen clearly in case of the sample taken from the transverse plane (Fig. 2a), and they look like tiny waves with regular arrangement and periods. On the other hand, the longitudinal plane is without these scratches (Fig. 3a)-almost ideally flat.

After the IO, the situation was similar for both samples. Figures 2b and 2c were taken from the transverse plane, from the internal oxidation zone (IOZ) and inner region, respectively. The Figure from the sample core (Fig. 2c) matches the Figure of the original material (Fig. 2a), while in the IOZ there are sprouts distributed equally through the whole zone. In Figures 3b and 3c, taken from the longitudinal plane, nanodomains of oxide are clearly and undoubtedly seen. They are bright in the original material matrix for the sample taken from the mantle region, and for the sample taken from the core just a few spots are hardly distinguishable.

After IO we obtained a one phase copper-aluminum solid solution in the core and finely dispersed oxide particles in the same matrix in the IOZ with a mean width of 2.6 nm.

The core of the sample remained one phase Cu-0.4%Al solid solution with slightly increased grains as a consequence of grain coarsening at higher temperatures. Contrary to this, in the IOZ precipitated oxide particles hindered the process of grain growth.

The application of ECAP leads to enormous differences between the planes, as well as zones for each plane. Figure 3d, taken from the IOZ of a longitudinal plane, shows us clear waves up to 300 nm high. We registered 3 wave-like shapes of 50 μm length. In the sample core (Fig. 3e), the wave height goes up to 500 nm, while their number is over 15 with 50 μm length. This points to the fact that the IOZ is harder and more deformation resistant than the sample

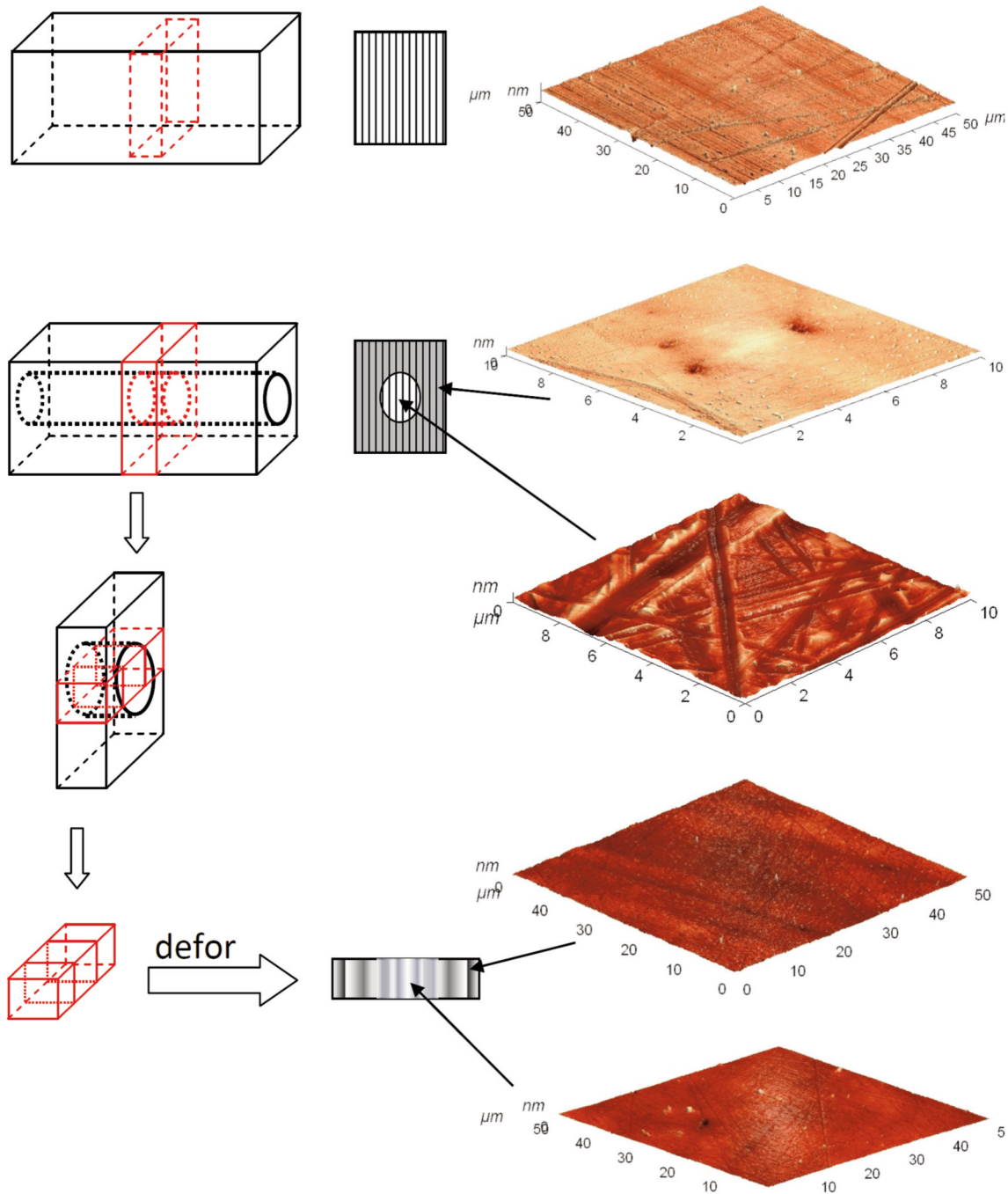


Figure 2. AFM picture of the Cu-0.4wt Al samples (transverse plane to the pressing direction).

core, where there was no oxidation.

For the transverse plane (Fig. 2), the situation is completely different. Amorphization of the sample seems to be greater. The figure taken from the IOZ (Figure 2d) shows a wave-like shape. However, it is very small and of insignificant height. In the sample core, Figure 2e, there is an almost flat area. Therefore,

the oxidation makes very big difference in the spectra. It is also obvious that the initial conditions, connected to the billet rolling, have a big influence on the final result. In both cases there is a clear difference in oxidation between the core and mantle region, but also the hardness and deformation degree show interesting and non-monotonous dependence.

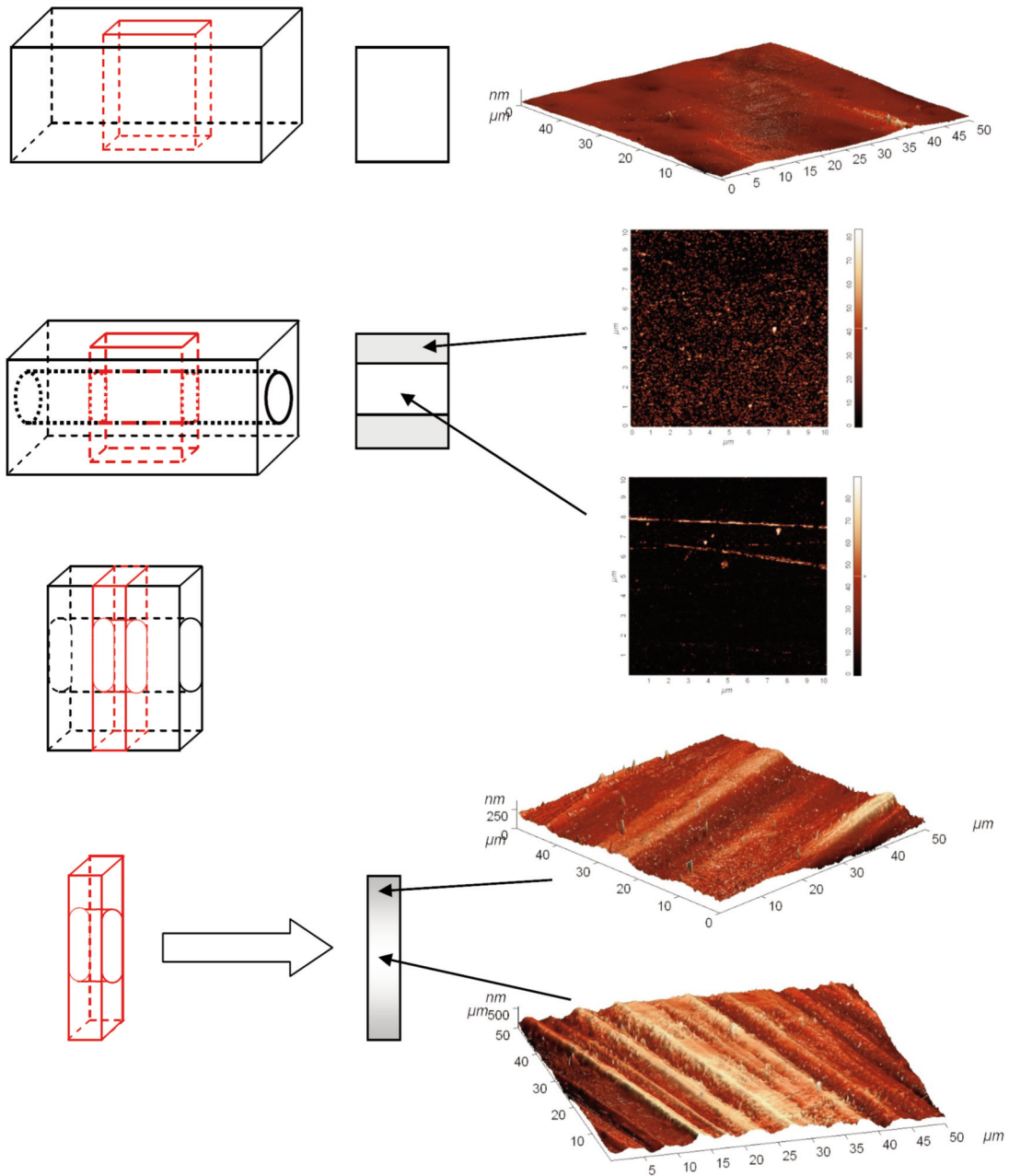


Figure 3. AFM picture of the Cu-0,4%wt Al samples (longitudinal plane to the pressing direction).

### 3.3. X-ray diffraction

The formation of phase and crystal structure of our samples after ECAP, both transversely and longitudinally to the pressing direction, were approved using the X-ray diffractometer, Model Philips PW 1050 diffractometer equipped with a PW 1730 generator, 40kV x 20mA, using Ni filtered  $\text{CoK}_\alpha$  radiation of 1.778897 Å at room temperature. Measurements were done in the  $2\theta$  range of 10-100°

with a scanning step of 0.05° and 10s scanning time per step.

Diffraction patterns obtained from the longitudinal plane (Figure 4) show clearly the diffraction maxima crystalline phases that crystallized in the cubic structure in the 225th space group Fm-3m in the Cu-structural type. In addition to these diffraction maxima, weak ones can be observed that can be joined at two phases (in the case of core Cu-0.4%wt. Al) or three phases (in the case of the IOZ of the Cu-0.4%wt.

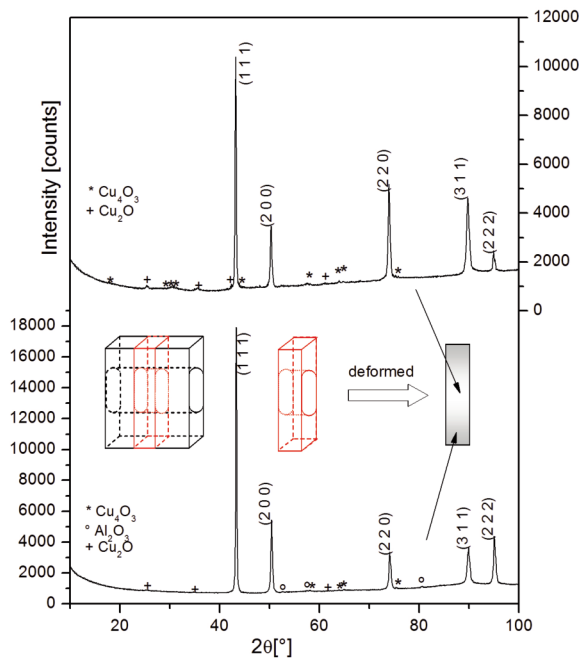


**Figure 4.** X-ray diffraction pattern of the Cu-0.4%wt Al samples after ECAP in a longitudinal plane to the pressing direction.

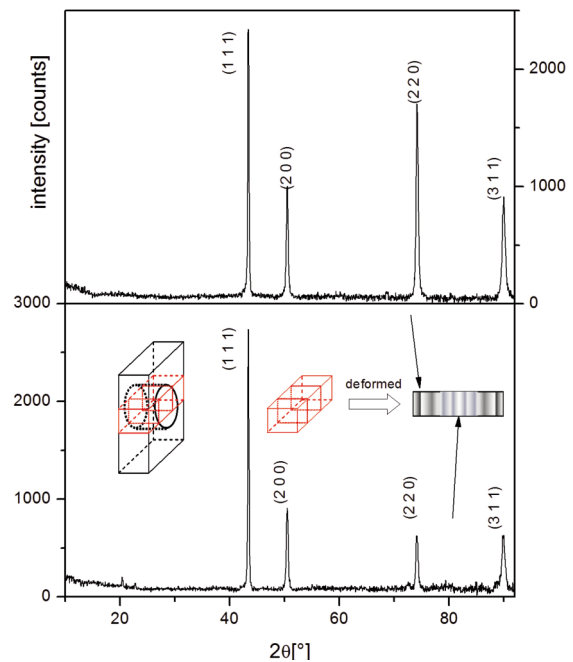


**Figure 5.** X-ray diffraction pattern of the Cu-0.4%wt Al samples after ECAP in a transverse plane to the pressing direction.

Al sample). These phases are  $\text{Cu}_4\text{O}_3$ ,  $\text{Cu}_2\text{O}$ ,  $\text{Al}_2\text{O}_3$  (diffraction maxima are indicated on diffraction). The presence of these phases in the sample is significant in the IOZ of our sample.

Diffraction patterns for the transverse plane are significantly different (Figure 5). Although in this case the same crystalline phase Cu is registered, the intensities are much less. After the clear maxima of metal copper, there is no presence of other phases in both samples. Also, from the relative ratio of clearly distinguished peaks one can tell that the sample taken from the IOZ shows preferable orientation in the (220) direction, while there is no such orientation in the sample core. This statement can be concluded for the longitudinal plane from Figure 4 as well.

### 3.4. Raman spectroscopy

The micro-Raman spectra were taken in the backscattering configuration and analyzed using a JobinYvon T64000 spectrometer, equipped with a nitrogen cooled charge-coupled-device detector. As an excitation source we used the 514.5nm line of an Ar-ion laser. The measurements were performed at 20mW laser power.

For analysis of the Raman spectra we assumed that all phonon lines were of the Lorentzian type, which is one of the common types of lines for this kind of analysis. Another common type of line is the Gaussian [8]. On Figs. 6 and 7 the obtained representative Raman spectra are presented. As we

have already mentioned, phases of Cu,  $\text{Cu}_2\text{O}$ ,  $\text{Cu}_3\text{O}_4$  and  $\text{Al}_2\text{O}_3$  were all registered by XRD. These phases can be nanodimensional, but also amorphous. For analysis of the vibration properties, in this case it is crucial to understand the vibrational properties of bulk materials, which is why we started the analysis of the obtained Raman spectra with a brief report about the structural and vibration properties of all potentially present phases in the sample. We expect that bulk modes would be shifted and broadened as a consequence of miniaturization or amorphization.

Pure copper has a face-centered cubic crystal structure and the first order of Raman active modes are not active.

CuO-based materials have been investigated extensively during the past two decades. In particular, the two main copper oxide phases, which are cupric oxide ( $\text{CuO}$ ) and cuprous oxide ( $\text{Cu}_2\text{O}$ ), are considered to be among the most important semiconductors. In addition, an interesting intermediate phase is paramelaconite,  $\text{Cu}_4\text{O}_3$ . In  $\text{Cu}_4\text{O}_3$ , which may be written as  $\text{Cu}_2^+\text{Cu}_2^{2+}\text{O}_3$ , copper is presented in both oxidation states: Cu(I) and Cu(II).

$\text{CuO}$  has monoclinic symmetry with the space group  $\text{C}_{2h}^6$  [9]. There are four Cu-O molecules per unit cell, and two Cu-O units in the primitive cell. The vibrational properties of  $\text{CuO}$  have been analyzed before using group theory and semi-empirical calculations [10].  $\text{CuO}$  has 12 phonon branches because there are four atoms in the primitive cell. A factor-group analysis gives the following zone-center

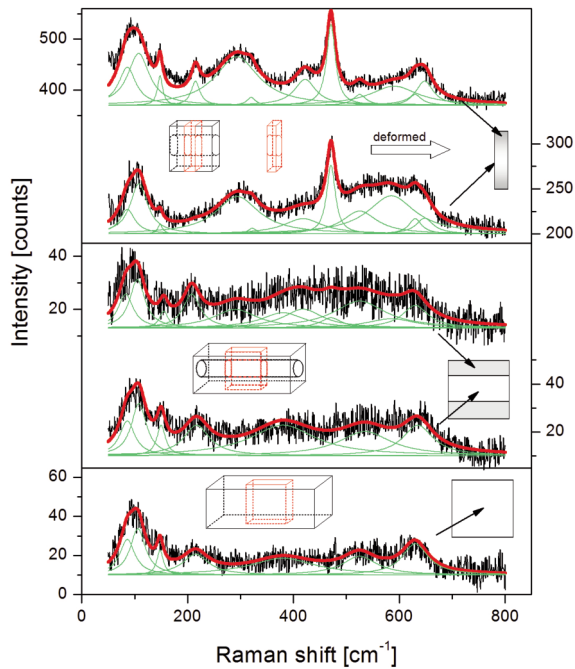


**Figure 6.** Raman spectra of the Cu-0,4%wt Al samples (longitudinal plane to the pressing direction).

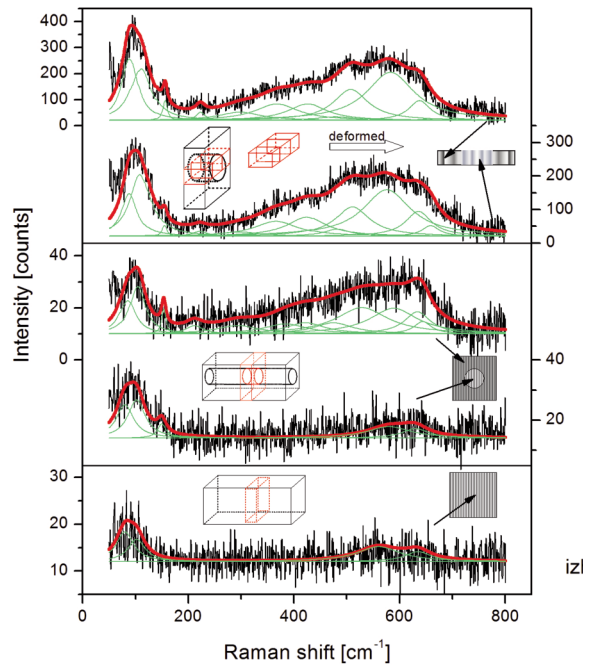


**Figure 7.** Raman spectra of the Cu-0,4%wt Al samples (transverse plane to the pressing direction).

modes:

$$\Gamma_{\text{vib}} = A_g + 2B_g + 4A_u + 5B_u \quad (1)$$

The three acoustic modes are  $A_u + 2B_u$  symmetry. Among the nine optical modes, three are Raman active ( $A_g + 2B_g$ ), and the remaining six are IR-active ( $3A_u + 3B_u$ ) [ $1\bar{1}\bar{1}$ ].

$\text{Cu}_2\text{O}$  crystallizes in a cubic lattice with two molecules per unit cell and space group  $\text{Pn}3\text{m}$ . Since it exhibits inversion symmetry, its electronic and vibrational states are of definite parity. The lattice dynamics of  $\text{Cu}_2\text{O}$  have also been studied by a number of workers [12, 13]. It can be shown that  $\text{Cu}_2\text{O}$  possesses three acoustic and 15 optical branches with symmetry  $F_{1u}$ , which are infrared active;  $F_{2g}$ , which is Raman active; and other symmetry - forbidden modes,  $F_{2u}$ ,  $A_{2u}$  and  $E_u$ , which in Raman scattering become allowed through an intrinsic selection-rule violating mechanism, and have been seen very near resonance with several exactions in  $\text{CuO}$  [14].

For the paramelaconite structure, group theory predicts 42 vibrational modes with the following irreducible representations at  $\Gamma$  - point of the Brillouin zone:

$$\Gamma_{\text{vib}} = 3E_g + A_{1g} + 2B_{1g} + 9E_u + 6A_{2u} + 5B_{2u} + 2B_{1u} + 2A_{1u} \quad (2)$$

$A_{2u} + E_u$  are the acoustic modes. All others are optical modes, among which nine are Raman active ( $A_{1g}$ ,  $B_{1g}$ , and  $E_g$ ), 21 are IR active ( $A_{2u}$  and  $E_u$ ) and nine are silent ( $A_{1u}$ ,  $B_{1u}$ , and  $B_{2u}$ ) [15].

It is well known [16] that  $\alpha\text{-Al}_2\text{O}_3$  belongs to the

$D_{3d}$  space group with two formula units of  $\text{Al}_2\text{O}_3$  per unit primitive cell of the trigonal system. The Al atoms are octahedrally coordinated with two layers of oxygen atoms. The octahedron is distorted severely. The irreducible representations for the optical modes in the crystal are:

$$\Gamma_{\text{vib}} = 2A_{1g} + 2A_{1u} + 3A_{2g} + 2A_{2u} + 5E_g + 4E_u \quad (3)$$

The irreducible representations for the acoustic modes are  $2A_{2u} + 1E_u$ . Since the unit cell has a center of symmetry, all first order Raman allowed vibrations are infrared forbidden and vice versa. More specifically, for corundum, vibrations with symmetry  $A_{1g}$  and  $E_g$  are Raman active and infrared inactive, while the  $A_{2u}$  and  $E_u$  vibrations are infrared active and Raman inactive. The  $A_{1u}$  and  $A_{2g}$  vibrations are inactive in both the infrared and Raman experiment. So,  $\alpha\text{-Al}_2\text{O}_3$  gives rise to seven Raman active modes  $2A_{1g} + 5E_g$  [17, 18].

The Raman spectra presented in Figures 6 and 7 can be described using the prior analysis, so the original sample, taken longitudinally to the pressing direction, can be reconstructed with 7 Lorentz profiles. The positions of these modes match  $\text{Cu}_2\text{O}$  vibrations ( $F_{2u}$  86  $\text{cm}^{-1}$ ,  $F_{1u}$  148  $\text{cm}^{-1}$ , multi-phonon 215  $\text{cm}^{-1}$ ,  $F_{2g}$  525  $\text{cm}^{-1}$  and  $F_{1u}$  630  $\text{cm}^{-1}$ ) and  $\alpha\text{-Al}_2\text{O}_3$  vibration ( $E_g$  (external) 380  $\text{cm}^{-1}$ ). All modes are broadened in comparison to the bulk crystal. For the sample taken from the core, it can be observed that there is no difference in the number of registered phonons before and after the IO. Registered phonons

are similar in line shape also, and all of them are shifted towards higher wavenumbers by a few  $\text{cm}^{-1}$ . In the sample taken from the mantle region new modes have appeared and they originate from:  $\text{CuO}$  ( $A_g$  290  $\text{cm}^{-1}$ );  $\text{Cu}_4\text{O}_3$  ( $B_g$  380  $\text{cm}^{-1}$ ,  $E_g$  471  $\text{cm}^{-1}$ ) and  $\alpha\text{-Al}_2\text{O}_3$  ( $A_{1g}$  (internal) 418  $\text{cm}^{-1}$ ,  $E_g$  585  $\text{cm}^{-1}$ ). Other phonons have less shifted positions than the phonons in the sample from the core, in comparison to the original material. Nevertheless, the main feature of these spectra is very low intensity. The useful signal does not go over 40 counts, which makes quantitative analysis much harder.

After the application of ECAP there is a distinctive rise of useful signal (about 3 times higher). In comparison with samples before ECAP, there is one new line that comes from  $\alpha\text{-Al}_2\text{O}_3$  ( $A_{1g}$  (internal) 648  $\text{cm}^{-1}$ ). However, a more important feature is the change in intensity of some lines. The dominant line in the spectrum is the one at 471  $\text{cm}^{-1}$  which comes from  $\text{Cu}_4\text{O}_3$ . This line has almost natural linewidth for bulk phonons, which indicates that there is a crystal structure of  $\text{Cu}_4\text{O}_3$  cluster. The phonon at 290  $\text{cm}^{-1}$  is enhanced and broadened. The integral intensity of this phonon in the sample from the mantle region is 3 times higher than the intensity in the sample from the core, and 15 times higher than before the application of ECAP. The intensity shift of the phonon at 420  $\text{cm}^{-1}$  is also interesting, while in the sample from the core there is no intensity shift, as expected, and in the sample from IOZ the intensity was changed by almost 4 times. The only phonon which was more intensive in the core material after the application of ECAP was the  $E_g$  phonon of  $\alpha\text{-Al}_2\text{O}_3$ . In the spectrum from the sample taken from the core, the multi-phonon from  $\text{Cu}_2\text{O}$  is missing.

The situation is different for the samples taken transversely to the pressing direction. The original sample has the simplest spectrum. Firstly, the useful signal is very weak and it is about 10 counts, which is on the border with noise. We can hardly distinguish the four modes which came from  $\text{Cu}_2\text{O}$  ( $F_{2u}$  80  $\text{cm}^{-1}$ ,  $E_u$  102  $\text{cm}^{-1}$  and  $F_{1u}$  635  $\text{cm}^{-1}$ ) and  $\alpha\text{-Al}_2\text{O}_3$  ( $E_g$  560  $\text{cm}^{-1}$ ). Phonon positions are shifted towards lower wavenumbers in comparison to the phonons in the longitudinal plane. Other phonons are probably in the noise and we were not able to detect them. After the IO the spectrum of the sample taken from the core stays almost unchanged. It seems that now the phonon  $\text{Cu}_2\text{O}$  ( $F_{1u}$  150  $\text{cm}^{-1}$ ) can be distinguished from the noise. The signal is a bit better in this spectrum, so that could be the reason for the appearance of this phonon. In sample from the IOZ there are the same phonons as registered for samples taken from the longitudinal plane, and the signals have similar intensities.

After the application of ECAP there were no drastic changes. The shape of the spectrum remained

the same without further appearance of a new line, as was the case for samples taken from the longitudinal plane. The most significant was the phonon of  $\alpha\text{-Al}_2\text{O}_3$  ( $E_g$  575  $\text{cm}^{-1}$ ), while its position in the sample taken from the core shifted to 560  $\text{cm}^{-1}$ . There is also a significant rise of intensity for phonon  $\text{Cu}_2\text{O}$  ( $F_{2g}$  525  $\text{cm}^{-1}$ ). The signal did rise 10 times after the application of ECAP, but the lines are broader, which indicates amorphization inside the sample.

## 5. Conclusions

In our research we investigated the microstructural characteristic of multiphase material based on internally oxidized Cu-0.4%wt Al that was subjected to the ECAP process. From the obtained results and their analyses several conclusions have been made:

With high temperature internal oxidation we obtained homogeneously distributed  $\text{Al}_2\text{O}_3$  particles in the coat region of the billet.

AFM measurements show clearly that the IOZ is harder and more deformation resistant than the sample core.

The obtained results indicated that the plastic deformation of the sample did lead to amorphization of the sample which might result from the increase in the free energy due to the high density of dislocations. This means that if the stored deformation energy increases upon straining, it is conceivable that transformation into the amorphous regime is energetically favorable.

The amorphization degree is bigger in the transversal plane than in the longitudinal plane.

The final sample has polyphase structure, and consists of Cu, CuO,  $\text{Cu}_2\text{O}$ ,  $\text{Cu}_4\text{O}_3$  and  $\square\text{Al}_2\text{O}_3$ . The phase arrangement is nonhomogenous, and it directly follows the technological process of making alloys.

## Acknowledgments

*This article has been supported by EUREKA Program ORTO-NITI E!6788 within the framework of the Ministry of Higher Education, Science and Technology of the Republic of Slovenia and by the European Union, European Social Fund for Young Researchers (TIA Agency). The work in Serbia was supported by Serbian Ministry of Education, Science and Technological Development under Project III45003.*

## References

- [1] I. Anžel, L. Kosec, A. C. Kneissl, *Microsc. Microanal.* 11(S02) (2005) 1692-1693.
- [2] R. K. Islamgaliev, W. Buchgraber, Y. R. Kolobov, N.M. Amirkhanov, A.V. Sergueeva, K.V. Ivanov, G.P. Grabovetskaya, *Mat. Sci. Eng. A* 319-321 (2001) 872-876.

- 
- [3] V.M. Segal, V.I. Reznikov, A.E. Drobyshevskiy, V.I. Kopylov, *Metally* 1 (1981) 99-105.
- [4] P.B. Prangnell, A. Gholinia, V.M. Markushev, in: T.C. Lowe, R.Z. Valiev (Eds.), *Investigations and Applications of Severe Plastic Deformation*, Kluwer Academic Pub., Dordrecht, 2000, pp. 65–71.
- [5] Y. Iwahashi, Z. Horita, M. Nemoto, T.G. Langdon, *Acta Mater.* 46 (1998) 3317-3331.
- [6] Y. Iwahashi, Z. Horita, M. Nemoto, T.G. Langdon, *Acta Mater.* 45 (1997) 4733-4741.
- [7] K. Nakashima, Z. Horita, M. Nemoto, and T.G. Langdon, *Mater. Sci. Eng. A281* (2000) 82-87.
- [8] H. Idink, V. Srikanth, W.B. While, and E.C. Subbarao, *J. Appl. Phys.* 76 (1994) 1819-1823.
- [9] S. Asbrink, L.J. Norrby, *Acta Crystallogr. Sect. B* 26 (1970) 8-15.
- [10] W. Reichardt, F. Gompf, M. Ain, B.M. Wanklyn, *Z. Phys. B* 81 (1990) 19-24.
- [11] G. Kliche, Z.V. Popovic, *Phys. Rev. B* 42 (1990) 10060-10066 and references therein.
- [12] Y. Petroff, P.Y. Yu, Y.R. Shen, *Phys. Rev. B* 12(6) (1975) 2488-2495.
- [13] C. Carabatos, and B. Prevot, *Phys. Status Solidi (b)* 37 (2) (1970) 773-779.
- [14] P.F. Williams and S.P.S. Porto, *Phys. Rev. B* 8 (4) (1973) 1782-1785.
- [15] L. Debbichi, M.C. Marco de Lucas, J.F. Pierson, P. Kruger, *J. Phys. Chem.* 116 (2012) 10232-10237.
- [16] P.G. Li, M. Lei, W.H. Tang, *Materials Letters*, 64 (2010) 161-163.
- [17] Y.Y. Chen, J. Hyltdoft, G.J.H. Jacobsen, O.F. Nielsen, *Spectrochim. Acta Part A* 51 (1995) 2161-9.
- [18] R. Krishnan, R. Kesavamoorthy, S. Dash, A.K. Tyagi, B. Raj., *Scr. Mater.* 48 (2103) 1099-1104.